Hydrol. Earth Syst. Sci. Discuss., 11, 9027–9066, 2014
www.hydrol-earth-syst-sci-discuss.net/11/9027/2014/
doi:10.5194/hessd-11-9027-2014

Hydrology and Earth System Sciences
Discussions
Open Access

Correction of systematic model forcing bias of CLM using assimilation of cosmic-ray neutrons and land surface temperature: a study in the Heihe catchment, China

X. Han[1,2], H.-J. Hendricks Franssen[2], R. Rosolem[3], R. Jin[1], X. Li[1], and H. Vereecken[2]

[1]Cold and Arid Regions Environmental and Engineering Research Institute, Chinese Academy of Sciences, Lanzhou, Gansu 730000, PR China
[2]Forschungszentrum Jülich, Agrosphere (IBG 3), Leo-Brandt-Strasse, 52425 Jülich, Germany
[3]Department of Civil Engineering, University of Bristol, Bristol BS8 1TR, UK

Received: 27 June 2014 – Accepted: 1 July 2014 – Published: 30 July 2014

Correspondence to: X. Han (hanxj@lzb.ac.cn)

Published by Copernicus Publications on behalf of the European Geosciences Union.

Abstract

The recent development of the non-invasive cosmic-ray soil moisture sensing technique fills the gap between point scale soil moisture measurements and regional scale soil moisture measurements by remote sensing. A cosmic-ray probe measures soil moisture for a footprint with a diameter of ~600 m (at sea level) and with an effective measurement depth between 12 and 76 cm, depending on the soil humidity. In this study, it was tested whether neutron counts also allow to correct for a systematic error in the model forcings. Lack of water management data often cause systematic input errors to land surface models. Here, the assimilation procedure was tested for an irrigated corn field (Heihe Watershed Allied Telemetry Experimental Research – HiWATER, 2012) where no irrigation data were available as model input although the area a significant amount of water was irrigated. Measured cosmic-ray neutron counts and Moderate Resolution Imaging Spectroradiometer (MODIS) land surface temperature (LST) products were jointly assimilated into the Community Land Model (CLM) with the Local Ensemble Transform Kalman Filter. Different data assimilation scenarios were evaluated, with assimilation of LST and/or cosmic-ray neutron counts, and possibly parameter estimation of leaf area index (LAI). The results show that the direct assimilation of cosmic-ray neutron counts can improve the soil moisture and evapotranspiration (ET) estimation significantly, correcting for lack of information on irrigation amounts. The joint assimilation of neutron counts and LST could improve further the ET estimation, but the information content of neutron counts exceeded the one of LST. Additional improvement was achieved by calibrating LAI, which after calibration was also closer to independent field measurements. It was concluded that assimilation of neutron counts was useful for ET and soil moisture estimation even if the model has a systematic bias like neglecting irrigation. However, also the assimilation of LST helped to correct the systematic model bias introduced by neglecting irrigation and LST could be used to update soil moisture with state augmentation.

HESSD
11, 9027–9066, 2014

1 Introduction

Soil moisture plays a key role for crop and plant growth, water resources management and land surface-atmosphere interaction. Therefore accurate soil moisture retrieval is important. Point scale measurements can be obtained by methods like time domain reflectometry (TDR) (Robinson et al., 2003) and larger scale, coarse soil moisture information from remote sensing sensors (Entekhabi et al., 2010; Kerr et al., 2010). Wireless Sensor Networks (WSN) allow characterization of soil moisture at the catchment scale with many local connected sensors at separated locations (Bogena et al., 2010). TDR only measures the point scale soil moisture and the maintenance of WSN is expensive. Recently, neutron count intensity measured by above-ground cosmic-ray probes was proposed as alternative information source on soil moisture. Neutron count intensity is measured non-invasively at an intermediate scale between the point scale and the coarse remote sensing scale (Zreda et al., 2008). A network of cosmic-ray sensors (CRS) has been set-up over N-America (Zreda et al., 2012).

Cosmic rays are composed of primary protons mainly. The fast neutrons generated by high-energy neutrons colliding with nuclei lead to "evaporation" of fast neutrons and the generated and moderated neutrons in the ground can diffuse back into the air where their intensity can be measured by the cosmic-ray soil moisture probe. Soil moisture affects the rate of moderation of fast neutrons, and controls the neutron concentration and the emission of neutrons into the air. Dry soils have low moderating power and are highly emissive; wet soils have high moderating power and are less emissive. The neutrons are mainly moderated by the hydrogen atoms contained in the soil water and emitted to the atmosphere where the neutrons mix instantaneously at a scale of hundreds of meters. The measurement area of a cosmic-ray soil moisture probe represents a circle with a diameter of ~ 600 m at sea level (Desilets and Zreda, 2013) and the measurement depth decreases non-linearly from ~ 76 cm (dry soils) to ~ 12 cm (saturated soils) (Zreda et al., 2008). The measured cosmic-ray neutron counts show an inverse correlation with soil moisture content. The cosmic-ray neutron intensity

HESSD
11, 9027–9066, 2014

could be reduced to 60 % of surface cosmic-ray neutron intensity if the soil moisture was increased from zero to 40 % (Zreda et al., 2008). The soil moisture estimation on the basis of cosmic-ray probe based neutron counts over a horizontal footprint of hectometers received considerable attention in scientific literature during the last years (Desilets et al., 2010; Zreda et al., 2008, 2012).

Hydrogen atoms are present as water in the soil, lattice soil water, below ground biomass, atmospheric water vapor, snow water, above ground biomass, intercepted water by vegetation and water on the ground. These additional hydrogen sources contribute to the measured neutron intensity. The role of these additional hydrogen sources should be included in the analysis of the cosmic-ray measurements in order to isolate the main contribution from soil moisture. Formulations for handling water vapor (Rosolem et al., 2013), for lattice water and organic carbon (Franz et al., 2013) and for a litter layer present on the soil surface (Bogena et al., 2013) have been developed.

It was shown that soil moisture measurements are useful for improving the soil moisture profile estimation in land surface models or hydrologic models (De Lannoy et al., 2007; Reichle, 2008; Yang et al., 2009). Assimilation of remotely sensed land surface temperature products also improves the estimation of evapotranspiration (Ghent et al., 2010; Reichle et al., 2010; Xu et al., 2011). In this paper we focus on the assimilation of measured cosmic-ray neutron counts for improving soil moisture content characterization at the field scale. The assimilation of measured cosmic-ray neutron counts in a land surface model has been tested (Han et al., 2014a; Rosolem et al., 2014; Shuttleworth et al., 2013). This paper focuses on the case that model input is biased. Land surface models still are affected by limited knowledge on water resources management and for regions in China (and elsewhere) typically no information on irrigation amounts is available as irrigation is mainly by the flooding system. We analyse whether measured neutron counts are able to correct for such biases. This case is not only relevant for neglecting irrigation in China, but also for other water resources management issues (e.g., groundwater pumping) which are neglected in the simulations. Neglecting irrigation in land surface models results in a large bias in the simulated soil moisture content because of a lack of water input. The bias in soil moisture content also results in a too small latent heat flux and too high sensible heat flux. We hypothesize that data assimilation also can play an important role for removing such biases in data deficient areas. One possible strategy in data assimilation studies for handling this type of bias, which is not followed in this paper, is to calibrate the simulation model (e.g., land surface model) prior to data assimilation to remove biases (Kumar et al., 2012) and use the corrected simulation model in the context of sequential data assimilation. A different strategy is followed in this paper and no a priori bias correction is carried out because this type of problem (neglecting water resources management) does not allow for such an a priori bias correction. Because the bias could be contributed to the model structure, model parameter, atmospheric forcing or observation data, and the bias-aware assimilation requires the assumption that the bias comes from a particular source (Dee, 2005). So the bias-blind assimilation was used for safety. Instead, it is investigated whether neutron counts measured by cosmic-ray probe are able to correct for the bias. Aim is to improve the soil moisture profile estimation in a crop land with seed corn as main crop type.

In CLM, the surface fluxes are calculated based on the Monin–Obukhov similarity theory. The sensible heat flux is formulated as a function of temperature and leaf area index, and the latent heat flux is formulated as a function of the temperature and leaf stomatal resistances. The leaf stomatal resistance is calculated from the Ball-Berry conductance model (Collatz et al., 1991). The surface fluxes are therefore sensitive to the surface and soil temperature. The land surface temperature (LST) products measured by the Moderate Resolution Imaging Spectroradiometer (MODIS) Terra (MOD11A1) and Aqua (MYD11A1) are also assimilated jointly to improve the soil temperature profile estimation because the evapotranspiration is sensitive to the soil temperature. Two Terra LST products can be obtained per day at 10:30 a.m./p.m. and two Aqua LST products can be obtained per day at 1:30 a.m./p.m. Soil moisture, land surface temperature and leaf area index contribute to the estimation of latent and sensible heat fluxes, and therefore this study focuses in addition on the calibration of

HESSD
11, 9027–9066, 2014

leaf area index. However, there are large discrepancies between the remotely retrieved LAI and measured values, and therefore the leaf area index is also calibrated by data assimilation. In summary, the novel aspects of this work are: (1) investigating whether data assimilation is able to correct for missing water resources management data without a priori bias correction; (2) joint assimilation of cosmic-ray neutron counts, LST and updating of LAI; (3) application of this framework to real-world data in an irrigated area with the availability of detailed verification data.

2 Materials and methods

2.1 Study area and measurement

The Heihe River Basin is the second largest inland river basin of China, and it is located between 97.1–102.0° E and 37.7–42.7° N and covers an area of approximately 143 000 km^2 (Li et al., 2013). In 2012, a multi-scale observation experiment of evapotranspiration with a well-equipped superstation (Daman superstation) to measure the atmospheric forcings and soil moisture at 2, 4, 10, 20, 40, 80, 120 and 160 cm depth (Xu et al., 2013), was carried out from June to September in the framework of the Heihe Watershed Allied Telemetry Experimental Research (HiWATER) (Li et al., 2013). SoilNet wireless network nodes (Bogena et al., 2010) were deployed to measure soil moisture content and soil temperature at four layers (4, 10, 20 and 40 cm). One cosmic-ray soil moisture probe (CRS-1000B) was installed (Han et al., 2014b) with 23 SoilNet nodes (Jin et al., 2014, 2013) in the footprint (Fig. 1). The main crop type within the footprint of the cosmic-ray probe is seed corn. The irrigation is applied through channels using the flooding irrigation method. Exact amounts of applied irrigation are therefore not available.

The measured cosmic-ray neutron count data were processed to remove the outliers according to the sensor voltage (≤ 11.8 V) and relative humidity (≥ 80 %). The surface fluxes were measured using the eddy covariance technique, and data were processed

HESSD
11, 9027–9066, 2014

using EdiRe (http://www.geos.ed.ac.uk/abs/research/micromet/EdiRe) software, in which the anemometer coordinate rotation, signal lag removal, frequency response correction, density corrections and signal de-spiking were done for the raw data. The energy balance closure was not considered in this study. The leaf area index was measured by the LAI-2000 scanner during the field experiment, there are 17 samples collected in 14 days of 3 months.

2.2 Land surface model and data

The Community Land Model (CLM) was used to simulate the spatio-temporal distribution of soil moisture, soil temperature, land surface temperature, vegetation temperature, sensible heat flux, latent heat flux and soil heat flux of the study area. The coupled water and energy balance are modeled in CLM, and the land surface heterogeneity is represented by patched plant functional types and soil texture (Oleson et al., 2013).

The soil properties used in CLM were from the soil database of China with 1 km spatial resolution (Shangguan et al., 2013). The MODIS 500 m resolution plant functional type product (MCD12Q1) (Sun et al., 2008) which was resampled by nearest neighbor interpolation to 1 km resolution and MODIS leaf area index product (MCD15A3) with 1 km spatial resolution (Han et al., 2012) were used as input. Due to a lack of measurement data, two atmospheric forcing data sets were used: the Global Land Data Assimilation System reanalysis data (Rodell et al., 2004) was interpolated using the National Centers for Environmental Prediction (NCEP) bilinear interpolation library iplib in spatial and temporal dimensions and used in the CLM for the spin-up period (http://www.nco.ncep.noaa.gov/pmb/docs/libs/iplib/ncep_iplib.shtml). For the three months data assimilation period forcing data from the Daman superstation of HiWATER were available and used.

HESSD
11, 9027–9066, 2014

2.3 Cosmic-ray forward model

In this study, the new developed COsmic-ray Soil Moisture Interaction Code (COSMIC) model (Shuttleworth et al., 2013) was used as the cosmic-ray forward model to simulate the cosmic-ray neutron count rate using the soil moisture profile as input. The effective measurement depth of the cosmic-ray soil moisture probe ranges from 12 cm (wet soils) to 76 cm (dry soils) (Zreda et al., 2008), within which 86 % of the above-ground measured neutrons originate. COSMIC also calculates the effective sensor depth based on the cosmic-ray neutron intensity and the soil moisture profile values (Franz et al., 2012; Shuttleworth et al., 2013).

COSMIC makes several assumptions to calculate the number of fast neutrons reaching the cosmic-ray soil moisture probe (N_{COSMOS}) at a near-surface measurement location, and the soil layer with a depth of 3 m for the complete soil profile, was discretized into 300 layers for the integration of Eq. (2) in COSMIC. The number of fast neutrons reaching the cosmic-ray probe N_{COSMOS} is formulated as (Shuttleworth et al., 2013):

$$N_{\mathrm{COSMOS}} = N \int_0^{\infty} \left\{ A(z)[\alpha \rho_{\mathrm{s}}(z) + \rho_{\mathrm{w}}(z)] \exp\left(-\left[\frac{m_{\mathrm{s}}(z)}{L_1} + \frac{m_{\mathrm{w}}(z)}{L_2} \right] \right) \right\} \mathrm{d}z \tag{1}$$

$$A(z) = \left(\frac{2}{\pi}\right) \int_0^{\pi/2} \exp\left(\frac{-1}{\cos(\theta)} \left[\frac{m_{\mathrm{s}}(z)}{L_3} + \frac{m_{\mathrm{w}}(z)}{L_4} \right] \right) \mathrm{d}\theta \tag{2}$$

$$\alpha = 0.405 - 0.102 \times \rho_{\mathrm{s}} \tag{3}$$

$$L_3 = -31.76 + 99.38 \times \rho_{\mathrm{s}} \tag{4}$$

where N is the high energy neutron intensity (counts h^{-1}), z denotes the soil layer depth (m), ρ_{s} denotes the dry soil bulk density (g cm^{-3}), ρ_{w} denotes the total water density, including the lattice water (g cm^{-3}) and α denotes the ratio of fast neutron

HESSD
11, 9027–9066, 2014

creation factor. L_1 is the high energy soil attenuation length with value of 162.0 g cm^{-2}, L_2 denotes the high energy water attenuation length of 129.1 g cm^{-2}. In Eq. (2) θ is the angle between the vertical below the detector and the line between the detector and each point in the plane, $m_s(z)$ and $m_w(z)$ are the integrated mass per unit area of dry soil and water (g cm^{-2}), respectively. L_3 denotes the fast neutron soil attenuation length (g cm^{-2}) and L_4 stands for the fast neutron water attenuation length with value of 3.16 g cm^{-2}.

The cosmic-ray neutron intensity reaching the land surface is influenced by air pressure, atmospheric water vapor content and incoming neutron flux. In order to isolate the contribution of soil moisture content to the measured neutron density, it is important to take these effects into account and the calibrated neutron count can be derived as follows:

$$N_{\mathrm{Corr}} = N_{\mathrm{Obs}} \cdot f_P \cdot f_{\mathrm{wv}} \cdot f_{\mathrm{i}} \tag{5}$$

where N_{Corr} represents corrected neutron counts and N_{Obs} the measured neutron counts. f_P is the correction factor for air pressure, f_{wv} the correction factor for atmospheric water vapor and f_{i} the correction factor for incoming neutron flux.

The correction factor for air pressure f_P can be calculated as (Zreda et al., 2012):

$$f_P = \exp\left(\frac{P - P_0}{L}\right) \tag{6}$$

where P (mbar) is the local air pressure, P_0 (mbar) the average air pressure during the measurement period and L (g cm^{-2}) is the mass attenuation length for high-energy neutrons; the default value of 128 g cm^{-2} was used for this study (Zreda et al., 2012).

The correction factor f_{wv} for atmospheric water vapor is calculated as (Rosolem et al., 2013):

$$f_{\mathrm{wv}} = 1 + 0.0054 \cdot \left(\rho_{\mathrm{v0}} - \rho_{\mathrm{v0}}^{\mathrm{ref}}\right) \tag{7}$$

HESSD
11, 9027–9066, 2014

where ρ_{v0} ($\mathrm{kg\,m^{-3}}$) is the absolute humidity at the measurement time and ρ_{v0}^{ref} ($\mathrm{kg\,m^{-3}}$) is the average absolute humidity during the measurement period.

Fluctuations in the incoming neutron flux should be removed because the cosmic-ray probe is designed to measure the neutron flux based on the incoming background neutron flux. The correcting factor f_i for the incoming neutron flux is calculated as:

$$f_i = \frac{N_m}{N_{avg}} \quad (8)$$

where N_m is the measured incoming neutron flux and N_{avg} is the average incoming neutron flux during the measurement period. The measured data at the Jungfraujoch station in Switzerland at 3560 m (http://cosray.unibe.ch/) was used to calculate N_m and N_{avg}.

In this study, the soil moisture at the CRS footprint scale was calculated from the arithmetic mean of the 23 SoilNet soil moisture observations. The calibration of the high energy neutron intensity parameter N in Eq. (1) was done using the measured cosmic-ray neutron counts rate and averaged soil moisture content at the CRS footprint scale. Because lattice water was unknown for this site, a value of 3 % was assumed in this study (Franz et al., 2012). Hourly soil moisture measurements for a period of 2.5 months were used for COSMIC calibration. Inside the cosmic-ray probe footprint, the amount of applied irrigation was spatially variable due to the different management practice of each farmer. The gradient search algorithm L-BFGS-B (Zhu et al., 1997) was used to minimize the root mean square error of the differences between simulated cosmic-ray neutron counts (using measured soil moisture by SoilNet as input to COSMIC) and the measured neutron counts N_{Corr}. The optimized parameter value of N was 615.96 counts $\mathrm{h^{-1}}$ in this case.

For the data assimilation, the simulated soil moisture content for 10 soil layers in CLM was used as the input to COSMIC in order to simulate the corresponding cosmic-ray neutron counts and compare it with the measured neutron counts. COSMIC calculates as output also the neutron count rate and the vertically weighted soil moisture content, which is calculated with help of the effective sensor depth obtained from COSMIC based on the vertical distribution of soil moisture contents.

2.4 Two source formulation – TSF

The land surface temperature products of MODIS are composed of a ground temperature and vegetation temperature component, which are however unknown. CLM models the ground temperature and vegetation temperature separately, but does not model the composed land surface temperature as seen by MODIS. The corresponding land surface temperature of CLM should therefore be modelled for data assimilation purposes. The two source formulation (Kustas and Anderson, 2009) was used in this study to calculate the land surface temperature from the MODIS view angle using ground temperature and vegetation temperature simulated by CLM:

$$T_\mathrm{s} = \left[F_\mathrm{c}(\Phi)T_\mathrm{c}^4 + \left(1 - F_\mathrm{c}(\Phi)T_\mathrm{g}^4\right)\right]^{1/4} \tag{9}$$

where T_s (K) is the composed surface temperature as seen by the MODIS sensor, $F_\mathrm{c}(\Phi)$ is the fraction vegetation cover observed from the sensor view angle Φ (radians), T_c (K) is the vegetation temperature and T_g (K) is the ground temperature (Kustas and Anderson, 2009):

$$F_\mathrm{c}(\Phi) = 1 - \exp\left(\frac{-0.5\Omega(\Phi)\mathrm{LAI}}{\cos\Phi}\right) \tag{10}$$

where LAI is the leaf area index, $\Omega(\Phi)$ is a clumping index to represent the nonrandom leaf area distributions of farmland or other heterogeneous land surfaces (Anderson et al., 2005), and is defined as:

$$\Omega(\Phi) = \frac{0.49\Omega_{max}}{0.49 + (\Omega_{max} - 0.49)\exp(k\theta^{3.34})} \tag{11}$$

$$\Omega_{max} = 0.49 + 0.51(\sin\Phi)^{0.05} \tag{12}$$

$$k = -\left\{0.3 + \left[1.7 \cdot 0.49 \cdot (\sin\Phi)^{0.1}\right]^{14}\right\} \tag{13}$$

2.5 Assimilation approach

The Local Ensemble Transform Kalman Filter (LETKF) was used as the assimilation algorithm, which is one of the square root variants of the ensemble Kalman filter (Evensen, 2003; Hunt et al., 2007; Miyoshi and Yamane, 2007). The model uncertainties are represented using the ensemble simulation of model states and LETKF derives the background error covariance using the model state ensemble members. LETKF uses the non-perturbed observations to update all the ensemble members of model states at each assimilation step.

In this study, $x_1^b,...,x_N^b$ denote the model state ensemble members; $\bar{x}^b$ is the ensemble mean of $x_1^b,...,x_N^b$; N is the ensemble size; $y_1^b,...,y_N^b$ denote the mapped model state ensemble members; $\bar{y}^b$ is the ensemble mean of $y_1^b,...,y_N^b$; H is the observation operator (COSMIC for soil moisture or the two source function for land surface temperature). The analysis step of LETKF can be summarized as follows:

Prepare the model state vector $\boldsymbol{X}^b$:

$$\boldsymbol{X}^b = \left[x_1^b - \bar{x}^b, ..., x_N^b - \bar{x}^b\right] \tag{14}$$

where $\bar{x}^b$ is composed of one vertically weighted soil moisture content and soil moisture content for 10 CLM-layers, resulting in a state dimension equal to 11 if only the neutron counts observations were assimilated; and $\bar{x}^b$ is composed of surface temperature,

HESSD
11, 9027–9066, 2014

Joint assimilation of cosmic-ray neutrons and land surface temperature

X. Han et al.

ground temperature, vegetation temperature and soil temperature for 15 CLM-layers if only the land surface temperature observations were assimilated without soil moisture update, giving a state dimension of 18. The water and energy balance are coupled, and in CLM the energy balance is firstly solved, then the derived surface fluxes are used in updating the soil moisture. So the cross correlation between the soil temperature and soil moisture could be calculated using the ensemble prediction in LETKF, and this makes the updating of soil moisture by assimilating land surface temperature possible. We also used the land surface temperature to update the soil moisture profile, in this case the soil moisture vector was augmented to the LETKF state vector of land surface temperature assimilation, and resulting in a state dimension of 28.

Construct the mapped model state vector $\boldsymbol{Y}^b$ after transformation of observation operator:

$$y_\mathrm{i}^b = H\left(x_\mathrm{i}^b\right) \tag{15}$$

$$\boldsymbol{Y}^b = \left[y_1^b - \bar{y}^b, \ldots, y_N^b - \bar{y}^b\right] \tag{16}$$

The following analysis is looped for each model grid cell to calculate the update of model state ensemble members:

Calculate analysis error covariance matrix $\mathbf{P}^\mathrm{a}$:

$$\mathbf{P}^\mathrm{a} = \left[(N-1)I + \boldsymbol{Y}^{bT}\mathbf{R}^{-1}\boldsymbol{Y}^b\right] \tag{17}$$

The perturbations in ensemble space are calculated as:

$$W^\mathrm{a} = \left[(N-1)\mathbf{P}^\mathrm{a}\right]^{1/2} \tag{18}$$

Calculate the analysis mean $\bar{w}^\mathrm{a}$ in ensemble space and add to each column of W^a to get the analysis ensemble in ensemble space:

$$\bar{w}^\mathrm{a} = \mathbf{P}^\mathrm{a}\boldsymbol{Y}^{bT}\mathbf{R}^{-1}(\boldsymbol{y}^\mathrm{o} - \bar{y}^b) \tag{19}$$

HESSD
11, 9027–9066, 2014

Calculate the new analysis:

$$X^{\mathrm{a}} = \boldsymbol{X}^{b}[\bar{w}^{\mathrm{a}} + W^{\mathrm{a}}] + \bar{x}^{b} \tag{20}$$

where **R** is the observation error covariance matrix, $\boldsymbol{y}^{\mathrm{o}}$ is the observation vector and X^{a} contains the updated model ensemble members.

The LETKF method can also be extended to do parameter estimation using a state augmentation approach (Bateni and Entekhabi, 2012; Li and Ren, 2011; Moradkhani et al., 2005; Nie et al., 2011). Alternative strategies for parameter estimation are a dual approach (Moradkhani et al., 2005) with separate updating of states and parameters. Vrugt et al. (2005) also proposed a dual approach with parameter updating in an outer optimization loop using Markov Chain Monte Carlo methods, and state updating in an inner loop. The a priori calibration of model parameters is also an option (Kumar et al., 2012). With the augmentation approach, the state vector of LETKF can be augmented by the parameter vector including soil properties (sand fraction, clay fraction and organic matter density) and vegetation parameters (leaf area index, etc.). In a preliminary sensitivity study it was found that for this site simulation results were more sensitive to the leaf area index than to soil properties. Soil texture is also quite well known for this site from measurements. Therefore in this study, only the leaf area index was in some of the simulation scenarios calibrated. In the different scenarios of land surface temperature assimilation, the LETKF state vector was also augmented to include leaf area index as calibration target. As a consequence, the augmented state vector contains surface temperature, ground temperature, and vegetation temperature, 15 layers of soil temperature and leaf area index, making up a state dimension equal to 19 for the scenarios of land surface temperature assimilation without soil moisture update; for the scenarios of land surface temperature with soil moisture update, the state dimension will be changed to 29.

HESSD
11, 9027–9066, 2014

3 Experiment setup

Firstly the 50 ensemble members of CLM with perturbed soil properties and atmospheric forcing data were driven from 1 January 2012 to 31 May 2012 to do the CLM spin-up; secondly an additional assimilation period of cosmic-ray neutron counts was done from 1 June 2012 to 30 August 2012 to reduce the spin-up error. Then the final CLM states on 30 August 2012 were used as the initial states for the following data assimilation scenarios. Perturbed soil properties were generated by adding a spatially uniform perturbation sampled from a uniform distribution between −10 and 10 % to the values extracted from the Soil Database of China for Land Surface Modeling (1 km spatial resolution). The leaf area index was perturbed with multiplicative uniform distributed random noise in the range of [0.8 ∼ 1.2]. The model forcings were perturbed by adding a perturbation, showing correlations in space and time. The spatial correlation was induced by a Fast Fourier Transform and the temporal correlation by a first-order auto-regressive model (Han et al., 2013; Kumar et al., 2009; Reichle et al., 2010). The statistics on the perturbation of the forcing data are summarized in Table 1.

The cosmic-ray neutron intensity was assimilated every 3 days at 12Z from the 1 June 2012 onwards, because we found that the difference between daily assimilation and 3 days assimilation was small (Entekhabi et al., 2010; Kerr et al., 2010). The measured neutron count intensity showed large temporal fluctuations in time and these fluctuations were not corresponding to the temporal variations of soil moisture. Therefore the measured neutron count intensity was smoothed with the Savitzky–Golay filter using a moving average window of size 31 h and a polynomial of order 4 (Savitzky and Golay, 1964). The originally measured neutron counts and smoothed neutron counts are plotted in Fig. 2. The assimilation frequency of MODIS LST products of MOD11A1 and MYD11A1 was up to 4 times (maximum) per day depending on the data availability. There are 230 observation data (including cosmic-ray probe neutron counts, MODIS LST, MOD11A1 and MYD11A1 LST) in the whole assimilation window.

HESSD
11, 9027–9066, 2014

The 4 days MODIS leaf area index product was aggregated and used as the CLM leaf area index parameter. Because the leaf area index from MODIS is usually lower than the true value (compared with the field measured leaf area index in the HiWATER experiment) and because the surface flux and surface temperature are sensitive to the leaf area index, two additional scenarios were investigated where leaf area index was calibrated to study the impact of leaf area index estimation on surface flux estimation within the data assimilation framework.

The following assimilation scenarios were compared: (1) CLM: open loop simulation without assimilation; (2) Only_CRS: only the measured neutron counts were assimilated; (3) Only_LST: only the MODIS LST products were assimilated. The quality control flags of LST products were used to select the data with good quality for assimilation; (4) CRS_LST: the measured neutron counts and MODIS LST products were assimilated jointly. In the above scenarios, the neutron count data was used to update the soil moisture and the LST data were used to update the ground temperature, vegetation temperature and soil temperature. (5) LST_Feedback: we also evaluated the scenario of assimilating the LST measurements to update the soil moisture profile. (6) CRS_LST_Par_LAI: the leaf area index was included as variable to be calibrated, otherwise the scenario was the same as CRS_LST. (7) LST_Feedback_Par_LAI: the leaf area index was included as variable to be calibrated, otherwise the scenario was the same as LST_Feedback. (8) CRS_LST_True_LAI: the in situ measured leaf area index during the HiWATER experiment was used in the model simulation.

HESSD
11, 9027–9066, 2014

4 Results and discussion

In order to evaluate the assimilation results for the different scenarios outlined in Sect. 3, the root mean square error (RMSE) was used:

$$\mathrm{RMSE} = \sqrt{\frac{\sum_{n=i}^{N} (\mathrm{Estimated}-\mathrm{Measured})^2}{N}} \tag{21}$$

where "Estimated" is the ensemble mean without assimilation or the ensemble mean after assimilation, "Measured" is measured soil moisture content evaluated at the SoilNet nodes (or latent heat flux, sensible heat flux or soil heat flux). N is the number of time steps. For the soil moisture analysis in this study, N is equal to 2184. The smaller the RMSE value is, the closer assimilation results are to measured values, which is in general considered to be desirable.

The temporal evolution of soil moisture content at 10, 20, 50 and 80 cm depth for different scenarios is plotted in Figs. 3 and 4. The RMSE values for different scenarios are summarized in Table 2. Assimilating the land surface temperature could improve the soil moisture profile estimation in the scenario of LST_Feedback_Par_LAI; the soil moisture results are better than the open loop run at all depths. With the assimilation of CRS neutron counts, the soil moisture RMSE values (scenarios CRS_LST_Par_LAI and CRS_LST_True_LAI) decreased significantly. The RMSE values for the scenarios Only_CRS and CRS_LST (not shown) are similar to CRS_LST_Par_LAI, which indicates that the main improvement for the soil moisture profile characterization is achieved by neutron count assimilation; and land surface temperature assimilation and leaf area index estimation play a minor role. Without assimilation of cosmic-ray probe neutron counts, the soil moisture simulation cannot be improved in the scenario Only_LST. However, the scenarios of LST_Feedback and LST_Feedback_Par_LAI improve the soil moisture profile characterization, which shows that explicitly using LST to update soil moisture content in the data assimilation routine gives better

HESSD
11, 9027–9066, 2014

results than using LST only to update soil moisture over the model equations. Results of LST_Feedback and LST_Feedback_Par_LAI are similar; therefore only results for LST_Feedback_Par_LAI are shown in Figs. 3 and 4. This implies that the improved soil moisture characterization due to LAI calibration is low. The results for the cosmic-ray probe neutron count assimilation proved the cosmic-ray probe sensor can be used to improve the soil moisture profile estimation at the footprint scale.

Figure 5 depicts the scatter plots of measured ET vs. modelled ET for different scenarios. The EC measured evapotranspiration (ET) is 384.7 mm for the assimilation period, without energy balance closure correction. The true evapotranspiration is therefore likely larger, but not much larger as the energy balance gap was limited (3.7 %). The CLM estimated ET, without data assimilation, using only precipitation as input is 223.7 mm and is much smaller than the measured value as applied irrigation is not considered in the model. This open loop simulated value would imply water stress and a limitation of canopy transpiration and soil evaporation due to low soil moisture content. Assimilation of land surface temperature only (Only_LST) hardly affected the estimated ET and was not able to correct for the artificial water stress condition. However, if land surface temperature was used to update soil moisture directly, taking into account correlations between the two states in the data assimilation routine, the ET estimates improved to 336.8 and 354.8 mm for the scenarios of LST_Feedback and LST_Feedback_Par_LAI respectively. The assimilation of land surface temperature of MODIS with soil moisture update results in significant improvements of ET.

The different neutron count assimilation scenarios also resulted in significantly improved estimates of ET. Univariate assimilation of cosmic-ray neutron data (Only_CRS) resulted in 301.9 mm ET. This shows that the impact of neutron count assimilation to correct evapotranspiration estimates is little smaller than the impact of land surface temperature with soil moisture update. Joint assimilation of land surface temperature data and cosmic-ray neutron data (CRS_LST) gave a slightly larger ET of 310.6 mm than Only_CRS. Scenarios of CRS_LST_Par_LAI and CRS_LST_True_LAI gave the best ET estimates (360.5 and 349.3 mm). This shows that correcting the biased LAI-estimates from MODIS by in situ data or calibration helped to improve model estimates.

The RMSE values of latent heat flux, sensible heat flux and soil heat flux for all scenarios are summarized in Figs. 6, 7, 8 and Table 3. It is obvious that the RMSE values are very large for both the latent heat flux (123.9 W m^{-2}) (Fig. 6) and sensible heat flux (80.5 W m^{-2}) (Fig. 7) for the open loop run and all other scenarios where the soil moisture was not updated. If the land surface temperature was assimilated to update the soil moisture, the latent heat flux RMSE decreased to 60.5 W m^{-2} (LST_Feedback) and 62.5 W m^{-2} (LST_Feedback_Par_LAI). Again, the assimilation of neutron counts also resulted in a strong RMSE reduction for the latent heat flux (76.5 W m^{-2} for Only_CRS). If in addition land surface temperature was assimilated and leaf area index optimized, the RMSE value of latent heat flux further decreased to 56.1 W m^{-2} (70.7 W m^{-2} without LAI optimization). If the field measured LAI was used instead in the assimilation (CRS_LST_True_LAI), the RMSE was 61.0 W m^{-2}. These results are in correspondence with the ones discussed before for soil moisture characterization. Evidently, the combined assimilation of cosmic-ray probe neutron counts and land surface temperature, and calibration of leaf area index (or use of field measured leaf area index as model input) shows the strongest improvement for the estimation of land surface fluxes. The soil heat flux did not show a clear improvement related to assimilation and showed only some improvement in case LAI was calibrated (Fig. 8). For the scenario of land surface temperature assimilation without soil moisture update (Only_LST), estimates of latent and sensible heat flux are not improved. It means that under water stress condition, the improved characterization of land surface temperature (and soil temperature) does not contribute to a better estimation of land surface fluxes.

The updated leaf area index for scenarios of LST_Feedback_Par_LAI and CRS_LST_Par_LAI is shown in Fig. 9. The MODIS leaf area index product was used as input for CLM and time series are plotted as blue line in Fig. 9 (Background). The leaf area index was also measured in the HiWATER experiment, and the measured values

HESSD
11, 9027–9066, 2014

are shown as green star (Observation). Ens_Mean represents the mean leaf area index of all ensemble members (Ensembles). It is obvious that MODIS underestimates the leaf area index compared with the observations. With the assimilation of land surface temperature, the leaf area index could be updated and be closer to the observations, but there is still a significant discrepancy between the measured leaf area index and the updated one. The leaf area index values for the scenario with leaf area index calibration (CRS_LST_Par_LAI) are close to the measured leaf area index values (CRS_LST_True_LAI), which is an encouraging result. The calibrated leaf area index shows some unrealistic increases and decreases during the assimilation period, which is inherent to the data assimilation approach. A smoothed representation of the leaf area index might provide a more realistic picture.

This study illustrates that for an irrigated farmland, the measured cosmic-ray probe neutron counts can be used to improve the soil moisture profile estimation significantly. Without irrigation data, CLM underestimated soil moisture content. The cosmic-ray neutron count data assimilation can be used as an alternative way to retrieve the soil moisture content profile in CLM. The improved soil moisture simulation was helpful for the surface flux characterization. The univariate assimilation of land surface temperature without soil moisture update is not helpful for the estimation of surface fluxes and even worsened the sensible heat flux characterization (Fig. 7). However, in a multivariate data assimilation framework where land surface temperature was assimilated together with measured cosmic-ray probe neutron counts, the land surface temperature assimilation contributed significantly to an improved ET estimation. The simulated canopy transpiration in CLM was in general too low, even when the water stress condition was corrected by assimilating neutron counts, which was related to small values of the leaf area index. The additional estimation of leaf area index through the land surface temperature assimilation resulted in an increase of the leaf area index yielding an increase of estimated ET.

In general, land surface models need to be calibrated before use in land data assimilation, especially if there is an apparent large bias in the model simulation (Dee,

HESSD
11, 9027–9066, 2014

2005). The simulation of soil moisture and surface fluxes was biased in our study, mainly due to the lack of irrigation water as input. This bias cannot be corrected a priori without exact irrigation data, which are not available in the field. The data assimilation was proven to be an efficient way to remove the model bias in this case. We also calculated the equivalent water thickness to analyze the equivalent irrigated water after each step of soil moisture update. For the scenarios of CRS_LST_Par_LAI and CRS_LST_True_LAI, the equivalent irrigation in three months was 693.6 and 607.6 mm, respectively. Because the irrigation method is flood irrigation, it is not easy to evaluate the true irrigation applied in the field. From the results we see however that the applied irrigation (in the model) is much larger than actual ET (~ 700 vs. ~ 400 mm). This could indicate that the amount of applied irrigation in the model is too large, but irrigation by flooding is also inefficient and results in excess runoff and infiltration to the groundwater, because it cannot be controlled so well as sprinkler irrigation or drip irrigation. Therefore, the calculated amount of irrigation could be realistic, but might also be too large if soil properties are erroneous in the model.

The soil moisture content measured by the cosmic-ray probe represents the depth between 12 cm (very humid) and 76 cm (extremely dry case) depending on the amount of soil water (soil moisture content and lattice water). Therefore the effective sensor depth of the cosmic-ray probe will change over time. In order to model the variable sensor depth and the relationship between the soil moisture content and neutron counts, the new developed COSMIC model was used as the observation operator in this study. Additionally the influences of air pressure, atmospheric vapor pressure and incoming neutron counts were removed from the original measured neutron counts. Because there is still some water in the crop which also affects the cosmic-ray probe sensor, the COSMIC observation operator could be improved to include vegetation effects. Several default parameters proposed by Shuttleworth et al. (2013) were used in the COSMIC model, these parameters probably need further calibration following the development of the COSMIC model.

The spatial distribution of soil moisture for the study area was very heterogeneous due to the small farmland patches and different irrigation periods for the different farmlands. Therefore the soil moisture content inferred by SoilNet may not represent the true soil moisture content of the cosmic-ray probe footprint, which is a further limitation of this study.

5 Summary and conclusions

In this paper, we studied the univariate assimilation of MODIS land surface temperature products, the univariate assimilation of measured neutron counts by the cosmic-ray probe, the bivariate assimilation of land surface temperature and neutron count data, and the additional calibration of leaf area index for an irrigated farmland at the Heihe catchment in China, where data on the amount of applied irrigation were lacking. The most important objective of this study was to test whether data assimilation is able to correct for the absence of information on water resources management as model input, a situation commonly encountered in large scale land surface modelling. For the specific case of lacking irrigation data, no a priori bias correction is possible. In case leaf area index was calibrated, this was done at each data assimilation step of land surface temperature. The data assimilation experiments were carried out with the Community Land Model (CLM) and the data assimilation algorithm used was the Local Ensemble Tranform Kalman Filter (LETKF). A likely further model bias, besides missing information on irrigation, is the underestimation of LAI by MODIS, which was used to force the model.

The results show that the direct assimilation of measured comic-ray neutron counts improves the estimation of soil moisture significantly, whereas univariate assimilation of land surface temperature without soil moisture update does not improve soil moisture estimation. However, if the land surface temperature was assimilated to update the soil moisture profile directly with help of the state augmentation method, the evapotranspiration and soil moisture could be improved significantly. This result

HESSD
11, 9027–9066, 2014

suggests that the land surface temperature remote sensing products are needed to correct the characterization of the soil moisture profile and the evapotranspiration. The improved soil moisture estimation after the assimilation of neutron counts resulted in a better ET estimation during the irrigation season, correcting the too low ET of the open loop simulation. The joint assimilation of neutron counts and MODIS land surface temperature improved the ET estimation further compared to neutron count assimilation only. The best ET estimation was obtained for the joint assimilation of cosmic-ray neutron counts, MODIS land surface temperature including calibration of the leaf area index (or if field measured leaf area index was used as input). This shows that bias due to neglected information on water resources management can be corrected by data assimilation if a combination of soil moisture and land surface temperature data is available.

We can conclude that data assimilation of neutron counts and land surface temperature is useful for ET and soil moisture estimation of an irrigated farmland, even if irrigation data are not available and excluded from model input. The land surface temperature measurements are an alternative data source to improve the soil moisture and land surface fluxes estimation under water stress conditions. This shows the potential of data assimilation to correct also a systematic model bias. Leaf area index optimization further improves simulation results, which is also likely related to a systematic underestimation of LAI by the MODIS remote sensing product. The results of using the calibrated leaf area index are comparable to the results of using field measured leaf area index as model input.

Acknowledgements. This work is supported by the NSFC (National Science Foundation of China) project (grant number: 41271357, 91125001), the Knowledge Innovation Program of the Chinese Academy of Sciences (grant number: KZCX2-EW-312) and the Transregional Collaborative Research Centre 32, financed by the German Science foundation. Jungfraujoch neutron monitor data were kindly provided by the Cosmic-ray Group, Physikalisches Institut, University of Bern, Switzerland. We acknowledge computing resources and time on the Supercomputing Center of Cold and Arid Region Environment and Engineering Research Institute of Chinese Academy of Sciences.

HESSD
11, 9027–9066, 2014

References

Anderson, M. C., Norman, J. M., Kustas, W. P., Li, F., Prueger, J. H., and Mecikalski, J. R.: Effects of vegetation clumping on two–source model estimates of surface energy fluxes from an agricultural landscape during SMACEX, J. Hydrometeorol., 6, 892–909, 2005.

Bateni, S. M. and Entekhabi, D.: Surface heat flux estimation with the ensemble Kalman smoother: joint estimation of state and parameters, Water. Resour. Res., 48, W08521, doi:10.1029/2011WR011542, 2012.

Bogena, H. R., Herbst, M., Huisman, J. A., Rosenbaum, U., Weuthen, A., and Vereecken, H.: Potential of wireless sensor networks for measuring soil water content variability, Vadose Zone J., 9, 1002–1013, 2010.

Bogena, H. R., Huisman, J. A., Baatz, R., Hendricks Franssen, H. J., and Vereecken, H.: Accuracy of the cosmic-ray soil water content probe in humid forest ecosystems: the worst case scenario, Water. Resour. Res., 49, 5778–5791, 2013.

Collatz, G. J., Ball, J. T., Grivet, C., and Berry, J. A.: Physiological and environmental-regulation of stomatal conductance, photosynthesis and transpiration – a model that includes a laminar boundary-layer, Agr. Forest Meteorol., 54, 107–136, 1991.

De Lannoy, G. J. M., Houser, P. R., Pauwels, V. R. N., and Verhoest, N. E. C.: State and bias estimation for soil moisture profiles by an ensemble Kalman filter: effect of assimilation depth and frequency, Water. Resour. Res., 43, W06401, doi:10.1029/2006WR005100, 2007.

Dee, D. P.: Bias and data assimilation, Q. J. Roy. Meteor. Soc., 131, 3323–3343, 2005.

Desilets, D. and Zreda, M.: Footprint diameter for a cosmic-ray soil moisture probe: theory and Monte Carlo simulations, Water. Resour. Res., 49, 3566–3575, 2013.

Desilets, D., Zreda, M., and Ferré, T. P. A.: Nature's neutron probe: land surface hydrology at an elusive scale with cosmic rays, Water Resour. Res., 46, W11505, doi:10.1029/2009WR008726, 2010.

Entekhabi, D., Njoku, E. G., O'Neill, P. E., Kellogg, K. H., Crow, W. T., Edelstein, W. N., Entin, J. K., Goodman, S. D., Jackson, T. J., Johnson, J., Kimball, J., Piepmeier, J. R., Koster, R. D., Martin, N., McDonald, K. C., Moghaddam, M., Moran, S., Reichle, R., Shi, J. C., Spencer, M. W., Thurman, S. W., Tsang, L., and Van Zyl, J.: The Soil Moisture Active Passive (SMAP) mission, P. IEEE, 98, 704–716, 2010.

Evensen, G.: The ensemble Kalman filter: Theoretical formulation and practical implementation, Ocean Dynam., 53, 343–367, 2003.

Franz, T. E., Zreda, M., Ferre, T. P. A., Rosolem, R., Zweck, C., Stillman, S., Zeng, X., and Shuttleworth, W. J.: Measurement depth of the cosmic ray soil moisture probe affected by hydrogen from various sources, Water. Resour. Res., 48, W08515, doi:10.1029/2012WR011871, 2012.

Franz, T. E., Zreda, M., Rosolem, R., and Ferre, T. P. A.: A universal calibration function for determination of soil moisture with cosmic-ray neutrons, Hydrol. Earth Syst. Sci., 17, 453–460, doi:10.5194/hess-17-453-2013, 2013.

Ghent, D., Kaduk, J., Remedios, J., Ardo, J., and Balzter, H.: Assimilation of land surface temperature into the land surface model JULES with an ensemble Kalman filter, J. Geophys. Res., 115, D19112, doi:10.1029/2010JD014392, 2010.

Han, X., Li, X., Hendricks Franssen, H. J., Vereecken, H., and Montzka, C.: Spatial horizontal correlation characteristics in the land data assimilation of soil moisture, Hydrol. Earth Syst. Sci., 16, 1349–1363, doi:10.5194/hess-16-1349-2012, 2012.

Han, X. J., Franssen, H. J. H., Li, X., Zhang, Y. L., Montzka, C., and Vereecken, H.: Joint assimilation of surface temperature and L-band microwave brightness temperature in land data assimilation, Vadose Zone J., 12, doi:10.2136/vzj2012.0072, 2013.

Han, X. J., Hendricks Franssen, H. J., Jiménez Bello, M. A., Rosolem, R., Bogena, H., Martínez Alzamora, F., Chanzy, A., and Vereecken, H.: Assimilation of cosmic-ray neutron counts for updating of soil moisture and soil properties with application to irrigation scheduling, J. Hydrol., submitted, 2014a.

Han, X. J., Jin, R., Li, X., and Wang, S. G.: Soil moisture estimation using cosmic-ray soil moisture sensing at heterogeneous farmland, IEEE Geosci Remote S., 11, 1659–1663, 2014b.

Hunt, B. R., Kostelich, E. J., and Szunyogh, I.: Efficient data assimilation for spatiotemporal chaos: a local ensemble transform Kalman filter, Physica D, 230, 112–126, 2007.

Jin, R., Wang, X., Kang, J., Wang, Z., Dong, C., and Li, D.: HiWATER: SoilNET Observation Dataset in the Middle Reaches of the Heihe River Basin, Heihe Plan Science Data Center, Lanzhou, doi:10.3972/hiwater.120.2013.db, 2013.

Jin, R., Li, X., Yan, B., Li, X., Luo, W., Ma, M., Guo, J., Kang, J., Zhu, Z., and Zhao, S.: A nested ecohydrological wireless sensor network for capturing the surface heterogeneity in the midstream areas of the Heihe River Basin, China, IEEE Geosci. Remote S., 11, 2015–2019, 2014.

Kerr, Y. H., Waldteufel, P., Wigneron, J. P., Delwart, S., Cabot, F., Boutin, J., Escorihuela, M. J., Font, J., Reul, N., Gruhier, C., Juglea, S. E., Drinkwater, M. R., Hahne, A., Martin-Neira, M., and Mecklenburg, S.: The SMOS mission: new tool for monitoring key elements ofthe global water cycle, P. IEEE, 98, 666–687, 2010.

Kumar, S. V., Reichle, R. H., Koster, R. D., Crow, W. T., and Peters-Lidard, C. D.: Role of subsurface physics in the assimilation of surface soil moisture observations, J. Hydrometeorol., 10, 1534–1547, 2009.

Kumar, S. V., Reichle, R. H., Harrison, K. W., Peters-Lidard, C. D., Yatheendradas, S., and Santanello, J. A.: A comparison of methods for a priori bias correction in soil moisture data assimilation, Water. Resour. Res., 48, W03515, doi:10.1029/2010WR010261, 2012.

Kustas, W. and Anderson, M.: Advances in thermal infrared remote sensing for land surface modeling, Agr. Forest Meteorol., 149, 2071–2081, 2009.

Li, C. and Ren, L.: Estimation of unsaturated soil hydraulic parameters using the ensemble Kalman filter, Vadose Zone J., 10, 1205–1227, 2011.

Li, X., Cheng, G. D., Liu, S. M., Xiao, Q., Ma, M. G., Jin, R., Che, T., Liu, Q. H., Wang, W. Z., Qi, Y., Wen, J. G., Li, H. Y., Zhu, G. F., Guo, J. W., Ran, Y. H., Wang, S. G., Zhu, Z. L., Zhou, J., Hu, X. L., and Xu, Z. W.: Heihe watershed allied telemetry experimental research (HiWATER): scientific objectives and experimental design, B. Am. Meteorol. Soc., 94, 1145–1160, 2013.

Miyoshi, T. and Yamane, S.: Local ensemble transform Kalman filtering with an AGCM at a T159/L48 resolution, Mon. Weather Rev., 135, 3841–3861, 2007.

Moradkhani, H., Sorooshian, S., Gupta, H. V., and Houser, P. R.: Dual state–parameter estimation of hydrological models using ensemble Kalman filter, Adv. Water Resour., 28, 135–147, 2005.

Nie, S., Zhu, J., and Luo, Y.: Simultaneous estimation of land surface scheme states and parameters using the ensemble Kalman filter: identical twin experiments, Hydrol. Earth Syst. Sci., 15, 2437–2457, doi:10.5194/hess-15-2437-2011, 2011.

Oleson, K., Lawrence, D. M., Bonan, G., Drewniak, B., Huang, M., Koven, C. D., Levis, S., Li, F., Riley, W. J., Subin, Z. M., Swenson, S. C., Thornton, P. E., Bozbiyik, A., Fisher, B. E. A., Kluzek, E., Lamarque, J. F., Lawrence, P. J., Leung, L. R., Lipscomb, W., Muszala, S., Ricciuto, D. M., Sacks, W., Sun, Y., Tang, J., and Yang, Z.-L.: Technical Description of Version 4.5 of the Community Land Model (CLM), Ncar Technical Note NCAR/TN-503+STR, National Center for Atmospheric Research, Boulder, CO, 422 pp., 2013.

HESSD
11, 9027–9066, 2014

Reichle, R. H.: Data assimilation methods in the Earth sciences, Adv. Water Resour., 31, 1411–1418, 2008.
Reichle, R. H., Kumar, S. V., Mahanama, S. P. P., Koster, R. D., and Liu, Q.: Assimilation of satellite-derived skin temperature observations into land surface models, J. Hydrometeorol., 11, 1103–1122, 2010.
Robinson, D. A., Jones, S. B., Wraith, J. M., Or, D., and Friedman, S. P.: A review of advances in dielectric and electrical conductivity measurement in soils using time domain reflectometry, Vadose Zone J., 2, 444–475, 2003.
Rodell, M., Houser, P. R., Jambor, U., Gottschalck, J., Mitchell, K., Meng, C. J., Arsenault, K., Cosgrove, B., Radakovich, J., Bosilovich, M., Entin, J. K., Walker, J. P., Lohmann, D., and Toll, D.: The global land data assimilation system, B. Am. Meteorol. Soc., 85, 381–394, 2004.
Rosolem, R., Shuttleworth, W. J., Zreda, M., Franz, T. E., Zeng, X., and Kurc, S. A.: The effect of atmospheric water vapor on neutron count in the cosmic-ray soil moisture observing system, J. Hydrometeorol., 14, 1659–1671, 2013.
Rosolem, R., Hoar, T., Arellano, A., Anderson, J. L., Shuttleworth, W. J., Zeng, X., and Franz, T. E.: Assimilation of near-surface cosmic-ray neutrons improves summertime soil moisture profile estimates at three distinct biomes in the USA, Hydrol. Earth Syst. Sci. Discuss., 11, 5515–5558, doi:10.5194/hessd-11-5515-2014, 2014.
Savitzky, A. and Golay, M. J. E.: Smoothing and differentiation of data by simplified least squares procedures, Anal. Chem., 36, 1627–1639, 1964.
Shangguan, W., Dai, Y., Liu, B., Zhu, A., Duan, Q., Wu, L., Ji, D., Ye, A., Yuan, H., Zhang, Q., Chen, D., Chen, M., Chu, J., Dou, Y., Guo, J., Li, H., Li, J., Liang, L., Liang, X., Liu, H., Liu, S., Miao, C., and Zhang, Y.: A China data set of soil properties for land surface modeling, J. Adv. Model. Earth Sy., 5, 212–224, 2013.
Shuttleworth, J., Rosolem, R., Zreda, M., and Franz, T.: The COsmic-ray Soil Moisture Interaction Code (COSMIC) for use in data assimilation, Hydrol. Earth Syst. Sci., 17, 3205–3217, doi:10.5194/hess-17-3205-2013, 2013.
Sun, W. X., Liang, S. L., Xu, G., Fang, H. L., and Dickinson, R.: Mapping plant functional types from MODIS data using multisource evidential reasoning, Remote Sens. Environ., 112, 1010–1024, 2008.
Xu, T. R., Liu, S. M., Liang, S. L., and Qin, J.: Improving predictions of water and heat fluxes by assimilating MODIS land surface temperature products into the common land model, J. Hydrometeorol., 12, 227–244, 2011.

HESSD
11, 9027–9066, 2014

Joint assimilation of cosmic-ray neutrons and land surface temperature

X. Han et al.

Xu, Z. W., Liu, S. M., Li, X., Shi, S. J., Wang, J. M., Zhu, Z. L., Xu, T. R., Wang, W. Z., and Ma, M. G.: Intercomparison of surface energy flux measurement systems used during the HiWATER-MUSOEXE, J. Geophys. Res., 118, 13140–13157, 2013.
Yang, K., Koike, T., Kaihotsu, I., and Qin, J.: Validation of a dual-pass microwave land data assimilation system for estimating surface soil moisture in semiarid regions, J. Hydrometeorol., 10, 780–793, 2009.
Zhu, C. Y., Byrd, R. H., Lu, P. H., and Nocedal, J.: Algorithm 778: L-BFGS-B: fortran subroutines for large-scale bound-constrained optimization, ACM T. Math. Software, 23, 550–560, 1997.
Zreda, M., Desilets, D., Ferre, T. P. A., and Scott, R. L.: Measuring soil moisture content non-invasively at intermediate spatial scale using cosmic-ray neutrons, Geophys. Res. Lett., 35, L21402, doi:10.1029/2008GL035655, 2008.
Zreda, M., Shuttleworth, W. J., Zeng, X., Zweck, C., Desilets, D., Franz, T., and Rosolem, R.: COSMOS: the COsmic-ray Soil Moisture Observing System, Hydrol. Earth Syst. Sci., 16, 4079–4099, doi:10.5194/hess-16-4079-2012, 2012.

Table 1. Summary of perturbation parameters for atmospheric forcing data.

Variables	Noise	Standard deviation	Time correlation scale	Spatial correlation scale	Cross correlation
Precipitation	Multiplicative	0.5	24 h	5 km	1.0, −0.8, 0.5, 0.0,
Shortwave radiation	Multiplicative	0.3	24 h	5 km	−0.8, 1.0, −0.5, 0.4,
Longwave radiation	Additive	$20\,W\,m^{-2}$	24 h	5 km	0.5, −0.5, 1.0, 0.4,
Air temperature	Additive	1 K	24 h	5 km	0.0, 0.4, 0.4, 1.0

HESSD
11, 9027–9066, 2014

Table 2. Root mean square error (RMSE) of soil moisture profile of open loop run (CLM), feedback assimilation of land surface temperature including LAI calibration (LST_Feedback_Par_LAI), bivariate assimilation of neutron counts and land surface temperature including LAI calibration (CRS_LST_Par_LAI) and bivariate assimilation of neutron counts and land surface temperature (CRS_LST_True_LAI).

Soil Layer Depth	RMSE ($m^3 m^{-3}$)			
	Open Loop (CLM)	LST_Feedback_Par_LAI	CRS_LST_Par_LAI	CRS_LST _True_LAI
10 cm	0.202	0.137	0.085	0.086
20 cm	0.167	0.106	0.047	0.048
50 cm	0.193	0.112	0.112	0.119
80 cm	0.188	0.124	0.136	0.146

HESSD
11, 9027–9066, 2014

Table 3. Root Mean Square Error (RMSE) of latent heat flux and sensible heat flux for different simulation scenarios.

Scenarios	RMSE ($W m^{-2}$)	
	Latent Heat	Sensible Heat
Open Loop (CLM)	123.9	80.5
LST_Feedback	60.5	34.8
LST_Feedback_Par_LAI	62.5	37.2
Only_CRS	76.5	43.3
CRS_LST	70.7	40.5
CRS_LST_Par_LAI	56.1	31.9
CRS_LST_True_LAI	61.0	34.5

HESSD
11, 9027–9066, 2014

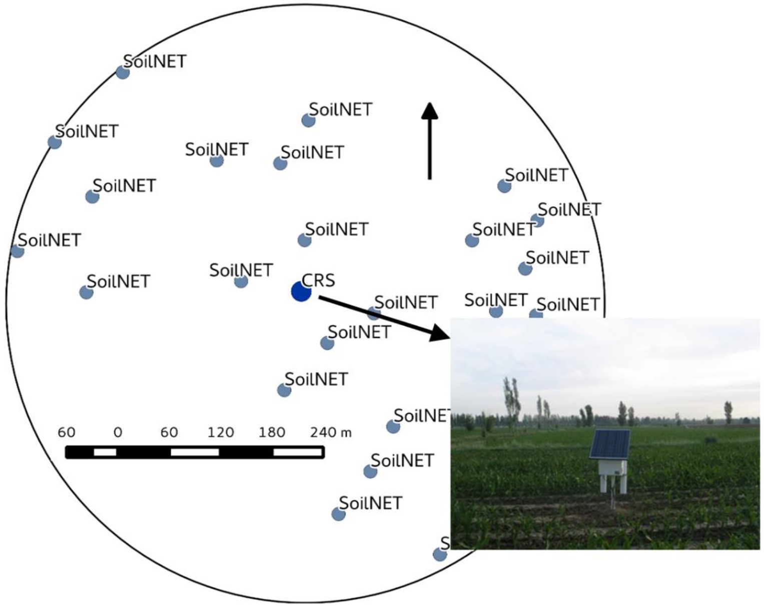

Figure 1. Map of the cosmic-ray probe and SoilNet Nodes in the footprint of the CRS probe positioned at the Heihe river catchment.

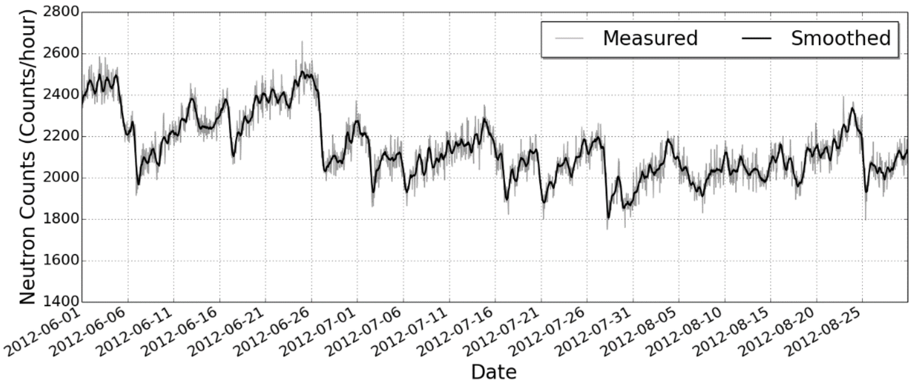

Figure 2. Measured and temporally smoothed CRS neutron counts.

HESSD
11, 9027–9066, 2014

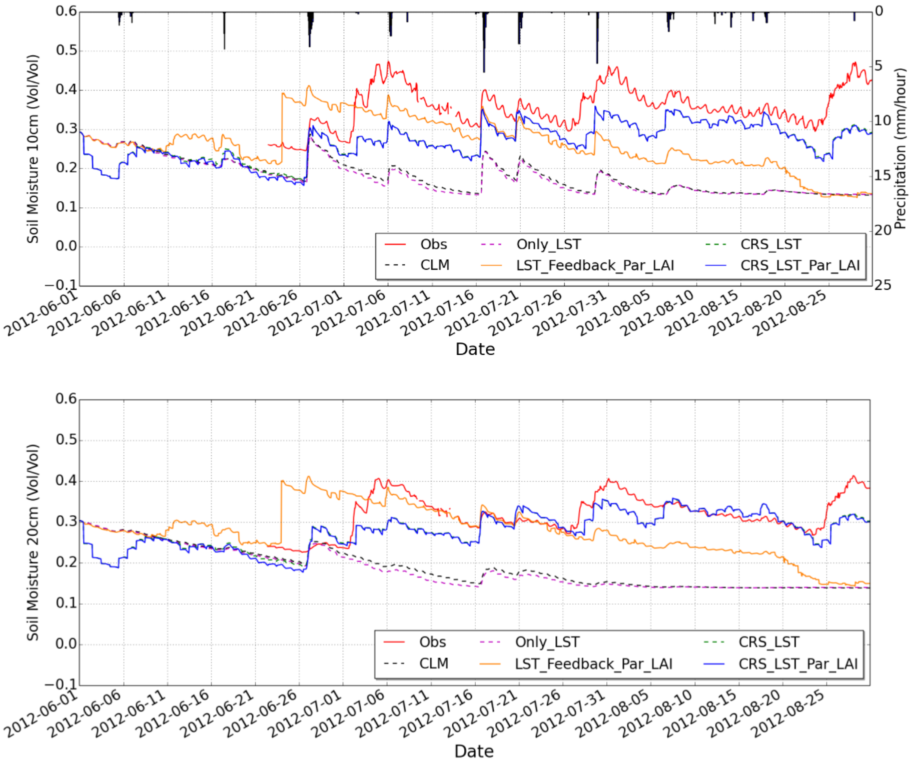

Figure 3. Soil moisture at 10 cm (upper) and 20 cm (lower) depth as obtained from an open loop run (CLM), local sensors (Obs), and different simulation scenarios. For a description of the scenarios see Sect. 3 of the paper. The CRS neutron counts were assimilated from 1 June.

HESSD
11, 9027–9066, 2014

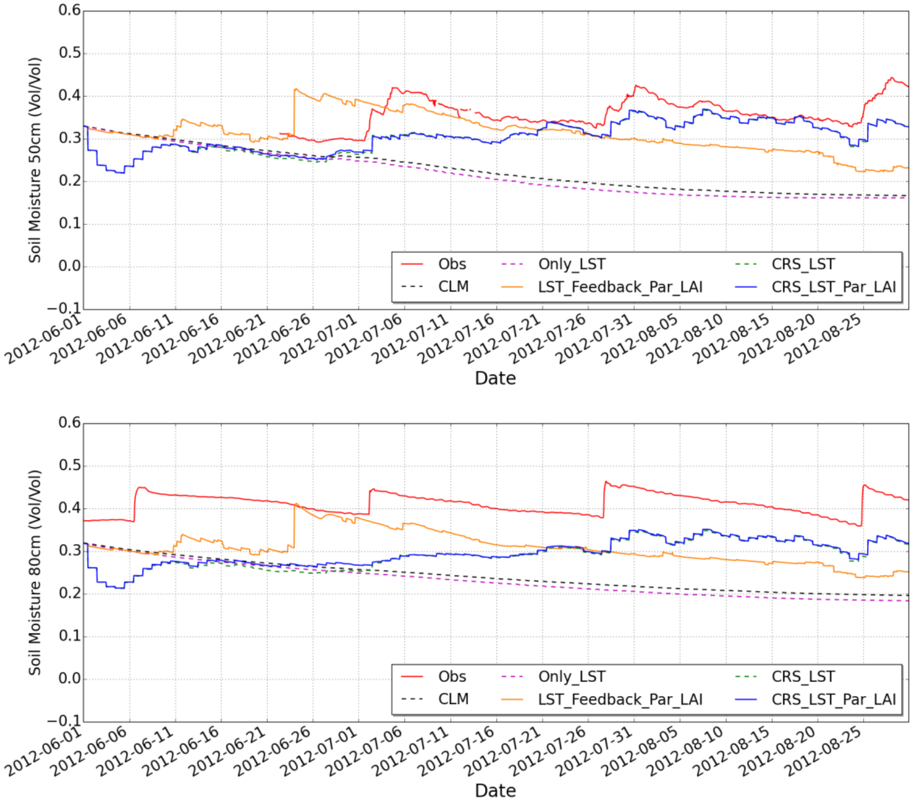

Figure 4. Soil moisture at 50 cm (upper) and 80 cm (lower) depth measured and modeled according different scenarios. For a full description see Fig. 3.

HESSD
11, 9027–9066, 2014

Joint assimilation of cosmic-ray neutrons and land surface temperature

X. Han et al.

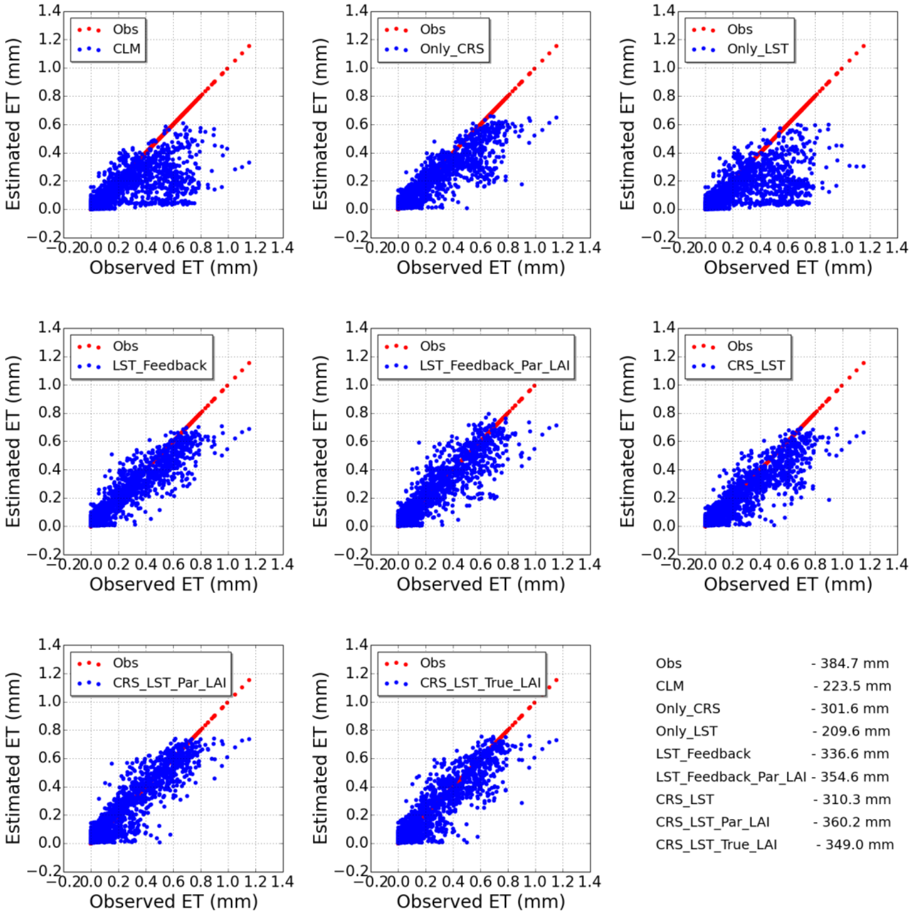

Figure 5. Evapotranspiration estimated according different scenarios for the period June–August 2012. For a full description see Fig. 3.

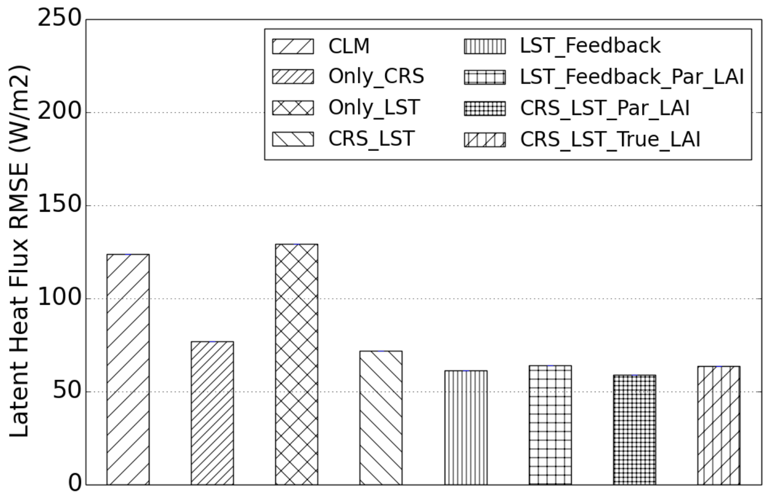

Figure 6. RMSE of latent heat flux for the period June–August 2012. For a description of the scenarios see Sect. 3 of the paper.

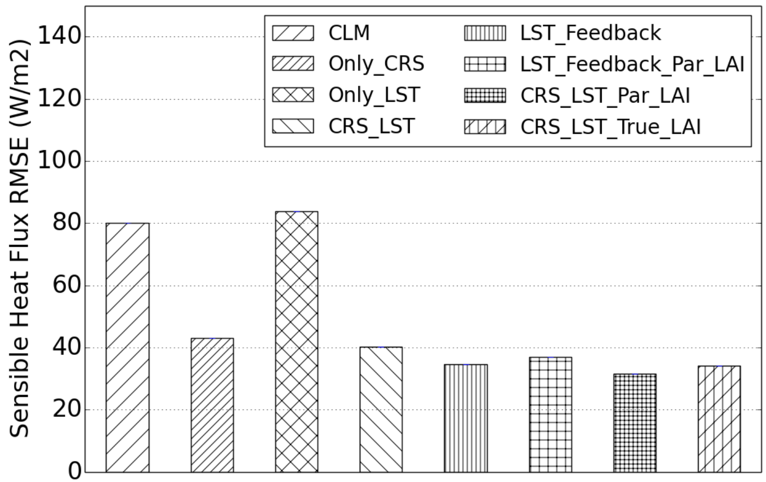

Figure 7. RMSE of sensible heat flux for the period June–August 2012. For a description of the scenarios see Sect. 3 of the paper.

HESSD
11, 9027–9066, 2014

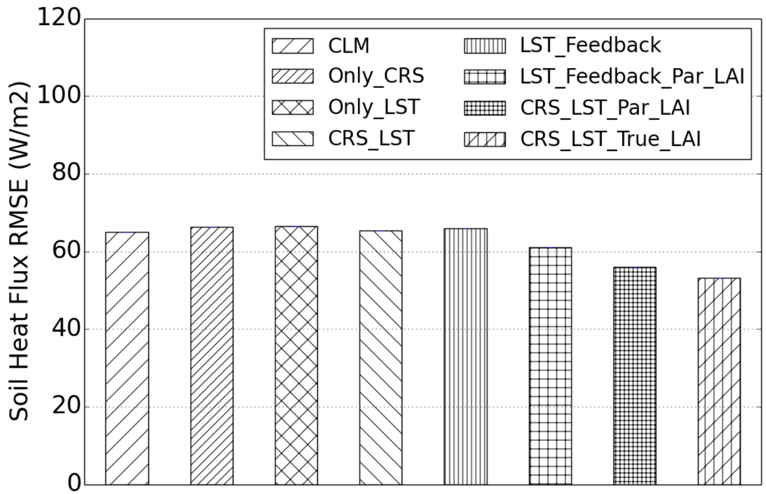

Figure 8. RMSE of soil heat flux for the period June–August 2012. For a description of the scenarios see Sect. 3 of the paper.

HESSD
11, 9027–9066, 2014

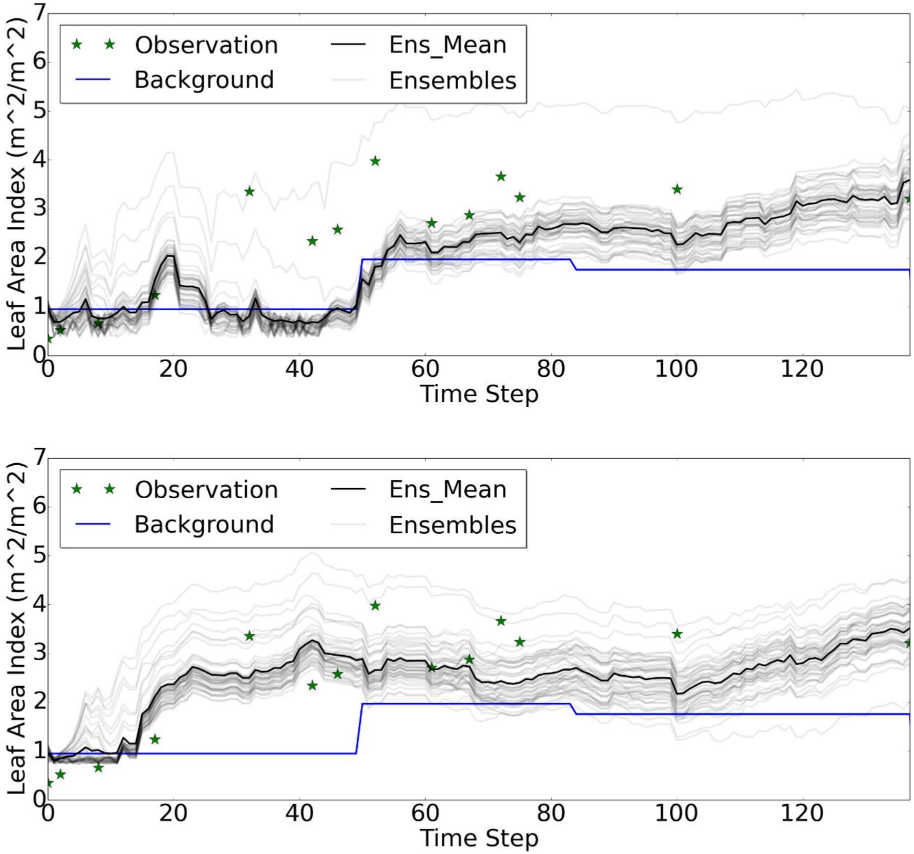

Figure 9. Leaf area index evolution for the period June–August 2012. Displayed are the measured leaf area index (Observation), default values (Background), mean of ensemble members (Ens_Mean) and ensemble members (Ensembles) for scenarios of LST_Feedback_Par_LAI (upper) and CRS_LST_Par_LAI (lower).